Molecular Therapy
Oncology
Original Article

AVL-armed oncolytic vaccinia virus promotes viral replication and boosts antitumor immunity via increasing ROS levels in pancreatic cancer

Jianlei Yu,[1] Nan An,[1] Jili Zhu,[1] Borong Zhu,[1] Guohui Zhang,[1] Kan Chen,[1] Yanrong Zhou,[1] Ting Ye,[1] and Gongchu Li[1]

[1]College of Life Sciences and Medicine, Zhejiang Sci-Tech University, Hangzhou 310018, China

Pancreatic malignant neoplasm is an extremely deadly malignancy well known for its resistance to traditional therapeutic approaches. Enhanced treatments are imperative for individuals diagnosed with pancreatic cancer (PC). Recent investigations have shed light on the wide-ranging anticancer properties of genetic therapy facilitated by oncolytic vaccinia virus. To illuminate the precise impacts of *Aphrocallistes vastus* lectin-armed oncolytic vaccinia virus (oncoVV-AVL) on PC, AsPC-1 and PANC-1 cells underwent treatment with oncoVV-AVL. Our findings revealed that oncoVV-AVL possesses the capacity to heighten oncolytic effects on PC cells and incite the production of diverse cytokines like tumor necrosis factor-α, interleukin-6 (IL-6), IL-8, and interferon-I (IFN-I), without triggering antiviral responses. Additionally, oncoVV-AVL can significantly elevate the levels of ROS in PC cells, initiating an oxidative stress response that promotes viral replication, apoptosis, and autophagy. Moreover, in xenograft tumor models, oncoVV-AVL notably restrained PC growth, enhanced IFN-γ levels in the bloodstream, and reprogrammed macrophages. Our investigation indicates that oncoVV-AVL boosts the efficacy of antitumor actions against PC tumors by orchestrating reactive oxygen species-triggered viral replication, fostering M1 polarization, and reshaping the tumor microenvironment to transform cold PC tumors into hot ones. These findings imply that oncoVV-AVL could present a novel therapeutic approach for treating PC tumors.

INTRODUCTION

Pancreatic cancer (PC) is a highly lethal malignancy with a low 5-year survival rate of only 11%.[1] Despite substantial advancements in treatment, the long-term survival rates for this disease have remained relatively poor. Surgical removal of the tumor is currently the primary therapy for PC, but its effectiveness has not shown significant improvement over time. One of the major challenges in effectively treating PC lies in diagnosing the disease at an early stage.[2] PC is often diagnosed at an advanced stage due to its deep-seated location behind the peritoneum and the asymptomatic nature in the early stages of the disease.[3,4] For patients who are unsuited for surgery, other therapeutic options, including radiotherapy, chemotherapy, and immunotherapy, are available. However, the effectiveness of these treatments is often constrained by factors, including tumor heterogeneity, dense tumor stroma, and drug resistance.[5–7] While immune-therapeutics, such as immune checkpoint inhibition, have shown promise as a new approach for malignant tumor therapy, PC has shown limited response to this type of therapy alone.[8] Hence, more effective treatments are needed for patients diagnosed with PC.

Oncolytic viruses (OVs) are a type of virus, either naturally occurring or genetically engineered, that can replicate selectively in and eliminate tumor cells while leaving normal cells unharmed.[9] Through innovative strategies, viruses have been transformed from latent pathogens into precisely engineered therapeutics that can enhance both direct viral-mediated attacks on cancer cells and secondary immune-mediated responses, offering a unique opportunity to finely tune and safely modulate the immune system's response for maximum antitumor efficacy.[10–14] Over the past few years, OVs have emerged as a potential and novel approach for treating PC. Clinical trials have investigated four main types of OVs in patients with PC, namely adenovirus, parvovirus, reovirus, and herpes simplex virus, demonstrating the potential clinical applications of OV therapy.[15] Vaccinia virus (VV) possesses several distinct advantages that make it a promising candidate for oncolytic virotherapy. These advantages include its rapid and efficient replication, ability to spread quickly from cell to cell within tumors, ability to infect cells without specific cellular receptors, a well-documented safety profile stemming from its historical use as a smallpox vaccine, cytoplasmic replication, natural tropism for tumors, and broad spectrum of cancer types it can target.[16–18] Multiple clinical trials involving VV-based OVs show safety and efficacy in diverse cancer types. For instance, Olvi-Vec, also known as GLV-1 h68 or GL-ONC1, which was engineered from the VV Lister strain with triple mutations in the J2R (thymidine kinase [TK]), F14.5 L, and A56R

Received 3 May 2024; accepted 10 September 2024;
https://doi.org/10.1016/j.omton.2024.200878.

Correspondence: Ting Ye, College of Life Sciences and Medicine, Zhejiang Sci-Tech University, Hangzhou 310018, China.
E-mail: yeting@zstu.edu.cn
Correspondence: Gongchu Li, College of Life Sciences and Medicine, Zhejiang Sci-Tech University, Hangzhou 310018, China.
E-mail: lgc@zstu.edu.cn

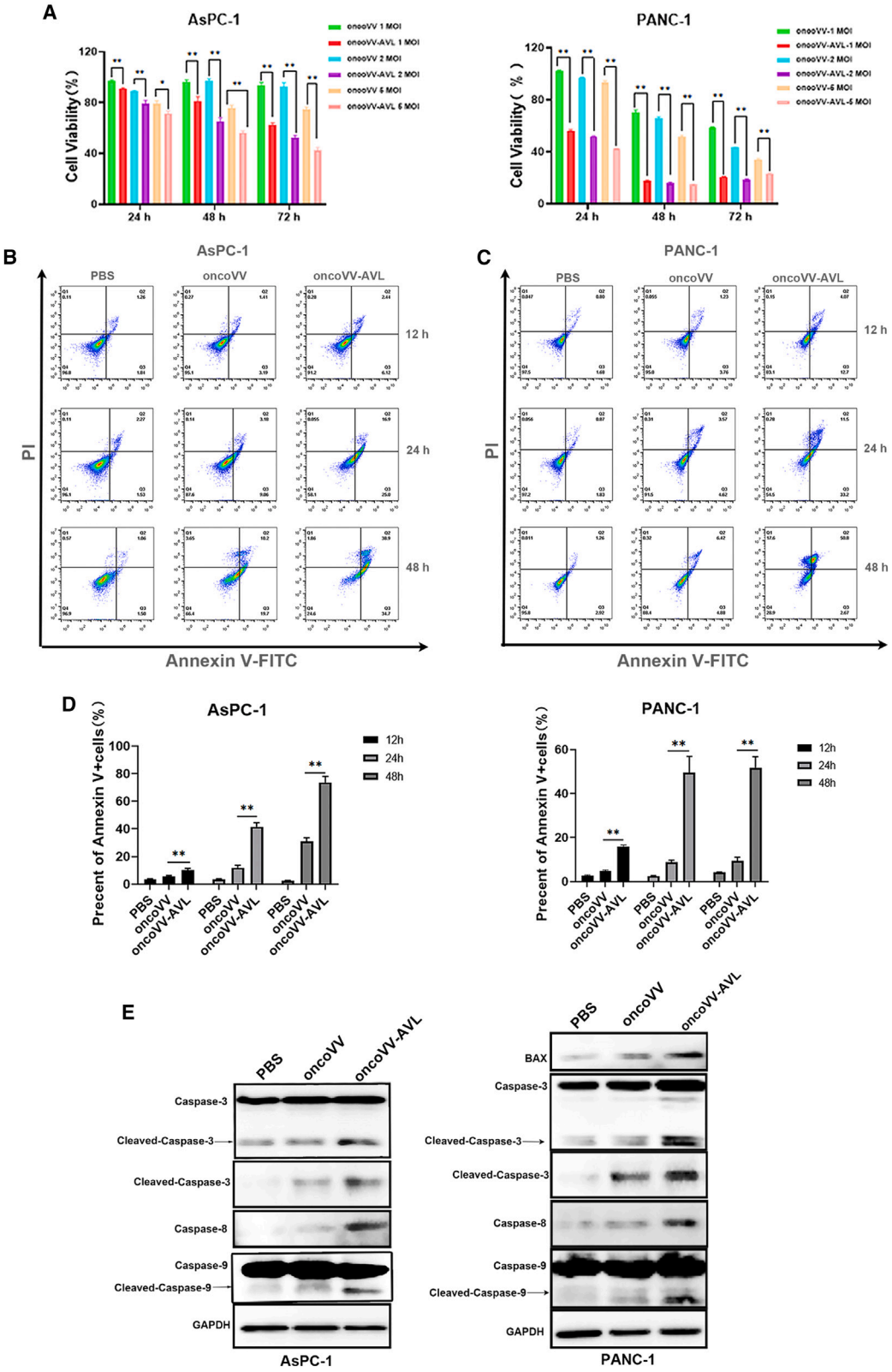

(legend on next page)

(hemagglutinin), followed by platinum-based chemotherapy with or without bevacizumab, displayed manageable safety and promising progression-free survival in patients with platinum-resistant or refractory ovarian cancer in this phase 2 nonrandomized clinical trial.[19] JX-594, an engineered VV derived from the Wyeth strain, armed with granulocyte-macrophage colony-stimulating factor and inactivated TK, in conjunction with low-dose cyclophosphamide and avelumab in a phase 2 trial, demonstrated safety and enhanced $CD8^+$ cell density, thereby altering the tumor microenvironment (TME) in soft tissue sarcomas.[20]

Lectins, as proteins capable of binding to carbohydrates, are found to be associated with various pathological processes.[21,22] Marine lectins, in particular, have shown promise in exerting antitumor effects by regulating cancer cell-signaling pathways, promoting apoptosis, inducing autophagy, and inhibiting angiogenesis.[23–25] In our previous work, we found that a series of OVs carrying marine lectins had effects on liver and breast cancers.[26–28] Notably, the oncoVV-equipped *Aphrocallistes vastus lectin* (AVL) gene (oncoVV-AVL), which undergoes homologous recombination by cloning AVL-FLAG into the plasmid pCB, resulting in inactivation of TK in the WR strain, shows promise as a potential cancer drug. Due to pancreatic malignancy being difficult to treat, marine lectins are unique in regulating the antitumor mechanism of OVs. We sought to shed light on the mechanisms underpinning the antitumor effect of oncoVV-AVL and to lay the groundwork for novel therapeutic strategies in the fight against PC.

Here, we evaluated the antitumor efficacy of oncoVV-AVL on PC in cell lines and xenograft tumor models. Furthermore, we sought to analyze the underlying mechanisms by which the virus influences apoptosis, autophagy, and viral replication in PC cells. Moreover, we investigated how oncoVV-AVL modulates the TME to identify new therapeutic strategies for treating PC.

RESULTS

OncoVV-AVL shows cytotoxic effect on PC cell lines

In our previous study, we confirmed that oncoVV-AVL could express AVL protein in human cells.[28] To evaluate the antitumor activity of oncoVV-AVL in PC cell lines, we conducted a thiazolyl blue tetrazolium bromide (MTT) colorimetry assay in AsPC-1 and PANC-1 cells after infection with OVs. In both cell lines, the cytotoxicity of the oncoVV-AVL group was notably higher over time than that of the oncoVV group. The data showed that oncoVV-AVL exhibited dose-related and time-dependent antitumor efficacy in AsPC-1 and PANC-1 cells (Figure 1A). We sought to investigate how oncoVV-AVL induces cytotoxicity, apoptosis rate of PC cells was determined utilizing flow cytometry 12, 24, and 48 h after infection. The results indicated that the apoptosis rate of PANC-1 cells treated with oncoVV-AVL increased from 16.77% to 53.47% post-infection from 12 to 48 h. The apoptosis rate of AsPC-1 cells infected with oncoVV-AVL increased from 8.56% to 73.6% and demonstrated that oncoVV-AVL substantially promoted cell apoptosis compared to the PBS and oncoVV groups (Figures 1B–1D). We further examined the apoptotic pathway in PANC-1 and AsPC-1 cells 36 h after viral infection using western blotting. The findings revealed pronounced activation of caspase-3, -8, and -9 in AsPC-1 cells in comparison to the oncoVV-treated group and activation of cleaved-caspase-3 and cleaved-caspase-9. Consistent results were illustrated in PANC-1 cells, with a notable rise in the expression level of Bax (Figure 1E). These data indicate that oncoVV-AVL exhibits great potency against PC cell lines.

OncoVV-AVL enhances viral replication

To determine whether oncoVV-AVL promotes viral replication, a $TCID_{50}$ (50% tissue culture infectious dose) assay was conducted to determine viral yields in PC cells. As depicted in Figures 2A and 2B, oncoVV-AVL exhibited markedly greater virus production than oncoVV. The protein A27L serves as a genetic marker for VV.[29] To further explore the impact of oncoVV-AVL on viral reproduction, we examined the expression of A27L in cells 36 h after infection with the virus. The results showed a marked increase in A27L expression in the oncoVV-AVL group. These findings suggest that AVL may boost the oncolytic effect of VV on PC cells by improving the replication capacity of the virus.

OncoVV-AVL promotes cytokine transcription in PC cells

Cytokines are crucial factors in cancer therapy. To investigate whether oncoVV-AVL induces the production of inflammatory cytokines, the expressions of tumor necrosis factor α (TNF-α), interleukins (IL-6, IL-8), and interferons (IFN-α/β, IFN-γ) were assessed via qPCR. The qPCR results revealed that the expressions of TNF-α, IL-6, IL-8, and IFN-α/β, and IFN-γ were upregulated upon infection with oncoVV-AVL in AsPC-1 cells (Figures 3A and 3C). Similarly, in PANC-1 cells, the levels of cytokine expressions were also elevated (Figures 3B and 3D).

To clarify the molecular mechanism driving the enhancement of type I IFN (IFN-I) expression by oncoVV-AVL, a dual-luciferase reporter gene assay was conducted to assess the transcriptional activities of AP-1 and IRF-3/7. The results illuminated that the transcriptional activities of AP-1, IRF-3, and IRF-7 were noticeably upregulated in the oncoVV-AVL treatment compared to the control in PC cells (Figures 4A–4C). This was further supported by western blotting analysis (Figures 4E and 4F), which showed increased phosphorylation of IRF-3/7 and the AP-1 components c-fos/c-jun in

Figure 1. The cytotoxic effect of oncoVV-AVL on pancreatic cancer cells

(A) Cytopathic effect of oncoVV-AVL *in vitro*. Cell viability was assessed in AsPC-1 and PANC-1 cells after infection with oncoVV or oncoVV-AVL at various MOIs of 1, 2, and 5 at 24 h, 48 h, and 72 h. Data are presented as the mean ± SD ($n = 5$). (B–D) Flow cytometry analyses of apoptosis. AsPC-1 (B) and PANC-1 (C) cells were infected with oncoVV or oncoVV-AVL for 12, 24, and 48 h. (E) Western blotting showing the expression of caspase-3/-8/-9, cleaved-caspase-3, and BAX in AsPC-1 and PANC-1 cells. GAPDH functioned as a loading control.

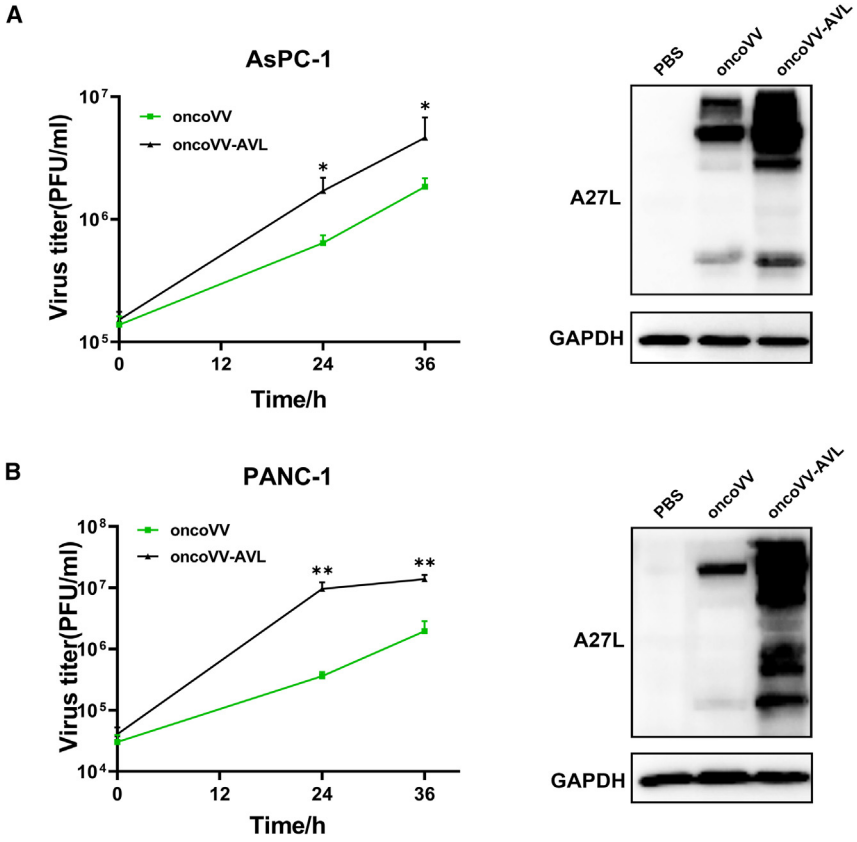

Figure 2. OncoVV-AVL promotes viral reproduction
(A) Viral yields in AsPC-1 and PANC-1 cells. (B) Cells were infected with oncoVV or oncoVV-AVL. Data are shown in mean ± SD (n = 3). Western blotting shows the expression of A27L in cells, with GAPDH serving as an internal reference.

oncoVV-AVL-infected cells, implying the activation of IRF-3/7 and AP-1 to initiate an inflammatory response.

The IFN-I stimulated response element (ISRE) binds the IFN-stimulated gene factor 3, inducing the transcription of over 300 IFN-stimulated genes that enhance the antiviral state.[30,31] Interestingly, the transcriptional activity of ISRE showed no significant changes in PC cells in the oncoVV-AVL group compared to those treated with PBS and oncoVV (Figure 4D), suggesting that while oncoVV-AVL enhances IFN production, it does not induce antiviral responses. Collectively, these discoveries support the hypothesis that oncoVV-AVL can activate transcription factors to enhance the cytokine transcription without eliciting antiviral responses, thereby enhancing the antitumor effects.

OncoVV-AVL promotes viral replication through eliciting autophagy

To ascertain the mechanism of oncoVV-AVL replication in PC cells, monodansylcadaverine (MDC) staining was used to detect autophagic vacuoles. The results displayed a significant shift in the staining peak of the oncoVV-AVL group (Figures 5A and 5B), indicating that oncoVV-AVL induces autophagy in AsPC-1 and PANC-1 cells. Furthermore, western blotting analysis in PC cells demonstrated that the oncoVV-AVL group displayed an appreciable increase in Beclin1 expression and an elevated ratio of LC3II/I, while showing a decrease in p62 expression (Figure 5C).

The PI3K-Akt-mTOR (phosphoinositol-Akt-mammalian target of rapamycin) pathway serves as the key upstream regulator of the autophagic pathway. Protein expression levels of PI3K and AKT were examined to assess their involvement in oncoVV-AVL-induced autophagy. The findings indicated that oncoVV-AVL activated the phosphorylation of PI3K and AKT, suggesting their role in promoting autophagy. We inferred that oncoVV-AVL enhances tumor cell autophagy to facilitate viral replication. To further investigate the influence of autophagy on viral replication, autophagy pathway inhibitors such as the PI3K inhibitor were utilized. The results demonstrated that the combination of oncoVV-AVL and 3-methyladenine (3-MA) notably reduced the viral replication ability in PC cells (Figure 5D). These findings provide additional evidence that AVL enhances viral replication through the autophagy pathway in PC cells.

OncoVV-AVL induces oxidative stress in PC cells

After treatment with oncoVV-AVL, reactive oxygen species (ROS) levels were increased remarkably in PC cells (Figure 6A). The nuclear factor erythroid 2-related factor 2 (Nrf-2) is known to be an inducible transcription factor that interacts with antioxidant response elements and regulates the upregulation of genes in response to oxidative stress.[32] We subsequently evaluated the expression levels of Nrf-2 in PC cells after 36 h of viral infection and observed a vast reduction in the expression levels of Nrf-2 in PC cells treated with oncoVV-AVL (Figure 6B). This suggests that oncoVV-AVL induces elevated ROS levels.

Next, we investigated how ROS levels affect tumor cell apoptosis. For this purpose, we treated with NADPH and NADH, which play a role in combating oxidative stress by maintaining glutathione and thioredoxin in a reduced state.[33] The results showed that when NADPH or NADH was added, the apoptosis rate of oncoVV-AVL-treated cells decreased (Figures 6C and 6D), and the expressions of caspase-3 and caspase-9, both involved in apoptosis, were downregulated (Figure 6E).

Several studies have shown that elevated ROS levels promote viral reproduction.[34–36] To support this hypothesis, we added NADPH or NADH to various treatment groups. After neutralizing high levels

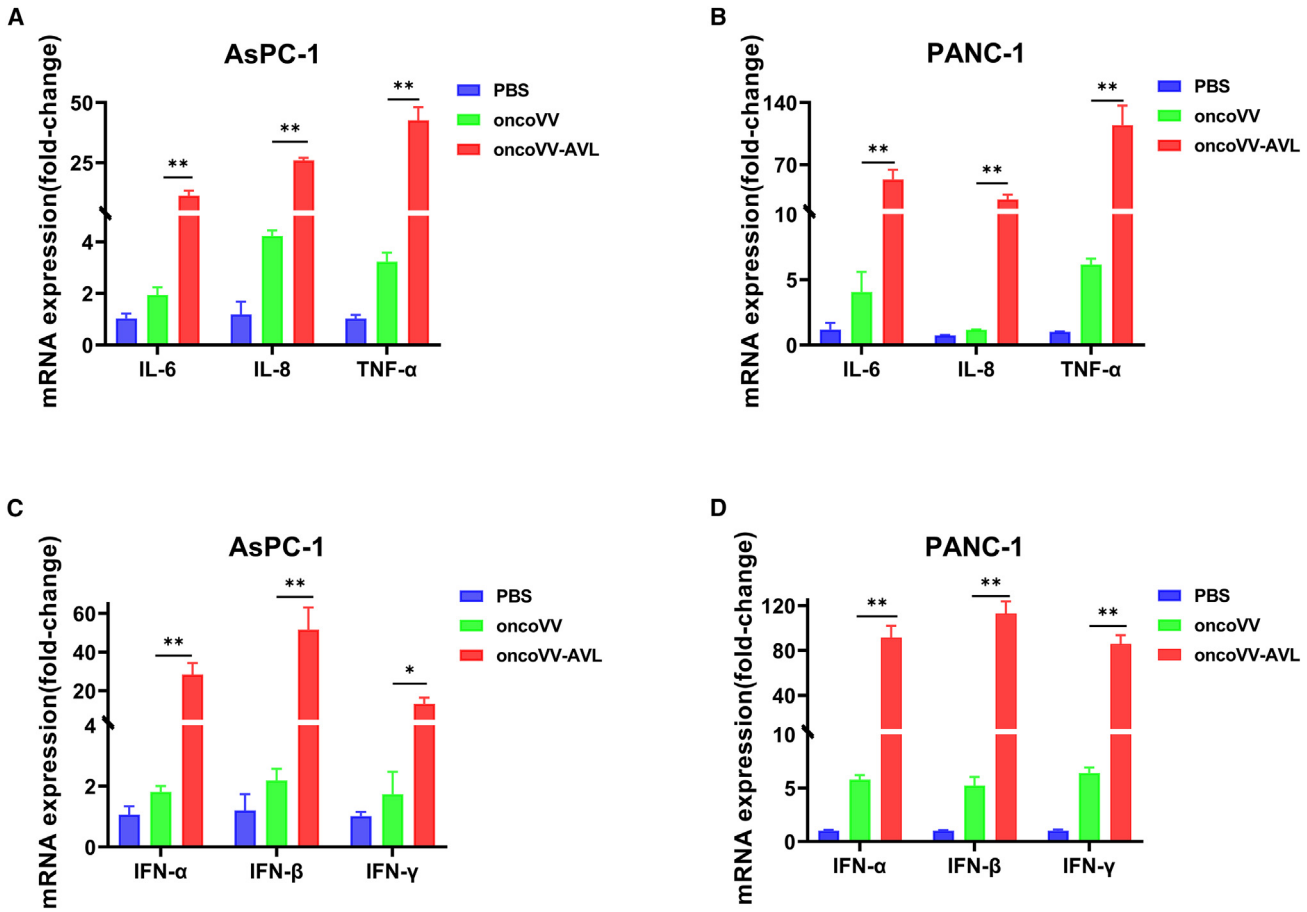

Figure 3. OncoVV-AVL enhances cytokine production in PC cells

(A and B) The mRNA levels of IL-6/-8 and TNF-α in AsPC-1 (A) and PANC-1 (B) cell lines. (C and D) The mRNA expression of IFN-α/-β/-γ in AsPC-1 (C) and PANC-1 (D) cell lines. The mRNA levels were detected by qPCR.

of ROS with NADPH or NADH, the viral yields of oncoVV-AVL treatment decreased (Figures 6F and 6G). OncoVV-AVL promotes viral replication and enhances antitumor efficiency by increasing ROS levels in PC cells.

OncoVV-AVL suppresses PC growth in the xenograft tumor model

To evaluate the therapeutic potency of oncoVV-AVL in pancreatic tumor xenograft mouse models, tumors were generated in BALB/c nude mice using AsPC-1 cells, and the established tumors were treated with either viruses or 0.9% NaCl on day 12. The results demonstrated that the oncoVV-AVL group exhibited a remarkable reduction in tumor volume compared to the groups treated with 0.9% NaCl or oncoVV alone, suggesting that oncoVV-AVL has a substantially greater impact on tumor regression than oncoVV treatment (Figures 7A–7C).

Although the decrease in tumor size from oncoVV-AVL treatment was not huge, pathological analysis reveals that a majority of the tissue has undergone necrosis. Histopathological analyses revealed pronounced karyorrhexis and coagulative necrosis specifically within the tumors treated with oncoVV-AVL, highlighting significant morphological alterations associated with oncoVV-AVL treatment compared to the other two groups (Figure 7D). Furthermore, western blotting assays demonstrated a notable increase in A27L expression in cells infected with oncoVV-AVL compared to those treated with oncoVV, suggesting that oncoVV-AVL promotes its oncolytic effects by enhancing viral replication, as evidenced by the elevated levels of A27L protein.

The combination of these observations suggests that oncoVV-AVL exhibits potent therapeutic efficacy in pancreatic tumor xenografts by enhancing viral replication to induce tumor regression.

OncoVV-AVL induces antitumor immunity *in vivo*

IFN-γ, a cytokine known as type II interferon and associated with antitumor immunity, has the potential to enhance the effectiveness of immunotherapy by activating immune cells within the tumor

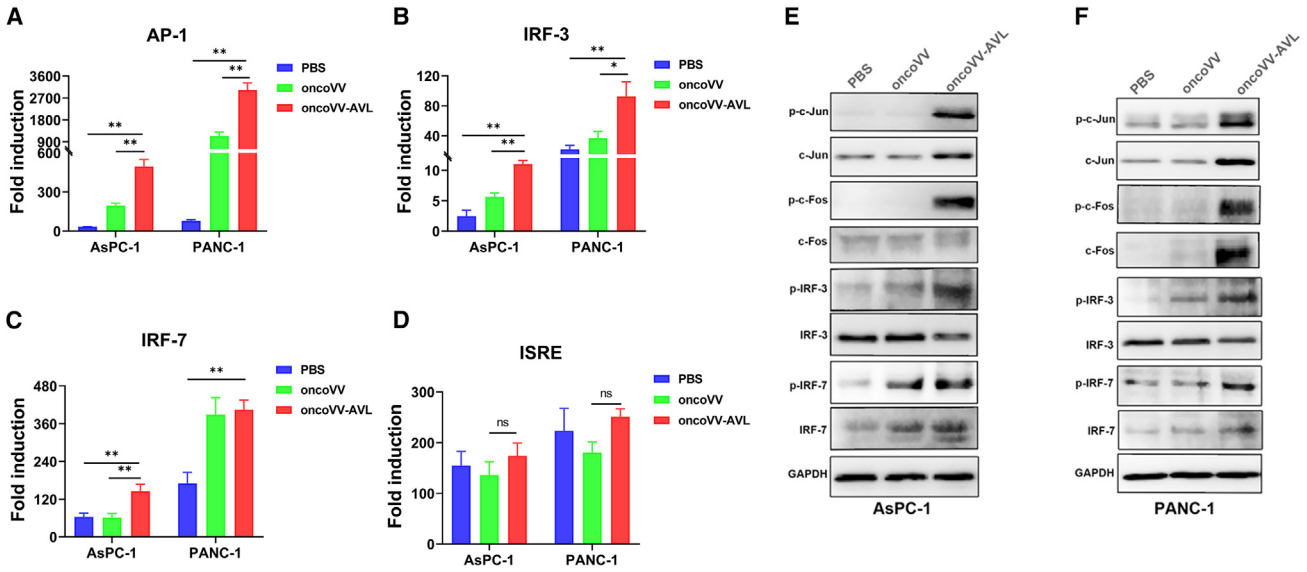

Figure 4. The oncoVV-AVL enhances the transcriptional activity of cytokines in PC cells and activates the cytokine synthesis pathway

(A–D) Transcriptional activity of AP-1 (A), IRF-3 (B), IRF-7 (C), and ISRE (D) in PANC-1 and AsPC-1 cells. Data are presented as the mean ± SD ($n = 3$). (E and F) The expression of c-Jun, c-Fos, p-c-Jun, p-c-Fos, IRF-3/-7, and *p*-IRF-3/-7 in AsPC-1 (E) and PANC-1 (F) cells. Western blotting was determined after cells were treated with oncoVV-AVL or oncoVV. GAPDH was used as an internal reference.

microenvironment.[37–41] In comparison to the oncoVV group, treatment with oncoVV-AVL resulted in significantly higher levels of serum IFN-γ, while there were no notable variances in serum IFN-β (Figures 8A and 8B). These observations demonstrate that oncoVV armed with AVL efficiently enhances the antitumor ability by modifying the tumor immune microenvironment. Furthermore, in the presence of NADPH, the treatment with oncoVV-AVL showed notably lower levels of serum IFN-γ compared to the oncoVV group (Figure 8A). This indicates that NADPH has the ability to neutralize ROS, thereby resulting in a reduction in inflammatory factors.

The TME exerts a significant influence on the advancement of tumors and their response to treatment, involving a diverse array of cell categories such as immune cells, lymphatics, endothelial cells, malignant cells, and stromal cells.[42–44] Tumor-associated macrophages (TAMs) can make up to 50% of certain solid tumors.[45] To assess the impact of treatment, we examined changes in macrophages using the F4/80 antibody and natural killer (NK) cells using the CD49b antibody.[46,47] As illustrated in Figure 8C, the findings indicated a roughly 36% increase in the proportion of M1 macrophages in the peritoneal exudate in the group treated with oncoVV-AVL compared to the group treated with oncoVV. The proportion of macrophages in myeloid cells was higher in the oncoVV-AVL treatment compared to the control group, while there were no notable differences in NK cells between the oncoVV-AVL group and the controls. The percentage of M2 macrophages (marked as IL-4$^+$ F4/80$^+$) remained constant without any alteration (Figure 8F). Additionally, there was a significant increase in the proportion of cells with both IFN-γ and F4/80 markers in the oncoVV-AVL treatment compared to the control group, indicating that oncoVV-AVL treatment can stimulate the proliferation of macrophage cells and drive them toward the M1 phenotype, resulting in an increased ratio of M1 to M2 macrophages (Figure 8G). These findings collectively indicate that oncoVV-AVL effectively enhances the polarization of TAMs into the M1 phenotype and activates antitumor immune responses within the TME *in vivo*.

To further verify that oncoVV-AVL boosts antitumor immunity in immunocompetent mice rather than in immunodeficient mice, we established a tumor-bearing mouse model by implanting Pan02 cells into C57BL/6 mice. The findings indicated that serum IFN-γ levels indeed rose in mice treated with oncoVV-AVL, yet no significant variance was observed in the control groups (Figure S1A). Additionally, the data showed a corresponding decline in serum IFN-γ levels when NADPH was present, suggesting that elevated ROS levels bolster antitumor immunity (Figure S1A). Furthermore, the study revealed an increase in the proportion of macrophages in the peritoneal exudate and myeloid cells of oncoVV-AVL-treated mice compared to controls, with no marked differences in NK cells between the oncoVV-AVL group and the 0.9% NaCl group within myeloid cells (Figures S1B and S1C). Similar trends were observed in C57BL/6 mouse models as in immunodeficient mice, where the quantity of macrophages and the ratio of M1 macrophages were higher in oncoVV-AVL-treated mice than in the control groups, while the percentage of M2 macrophages remained relatively stable across different treatments (Figures S1D–S1F). These results suggest that oncoVV-AVL effectively promotes the polarization of TAMs toward the M1 phenotype in tumor-bearing immunocompetent mice.

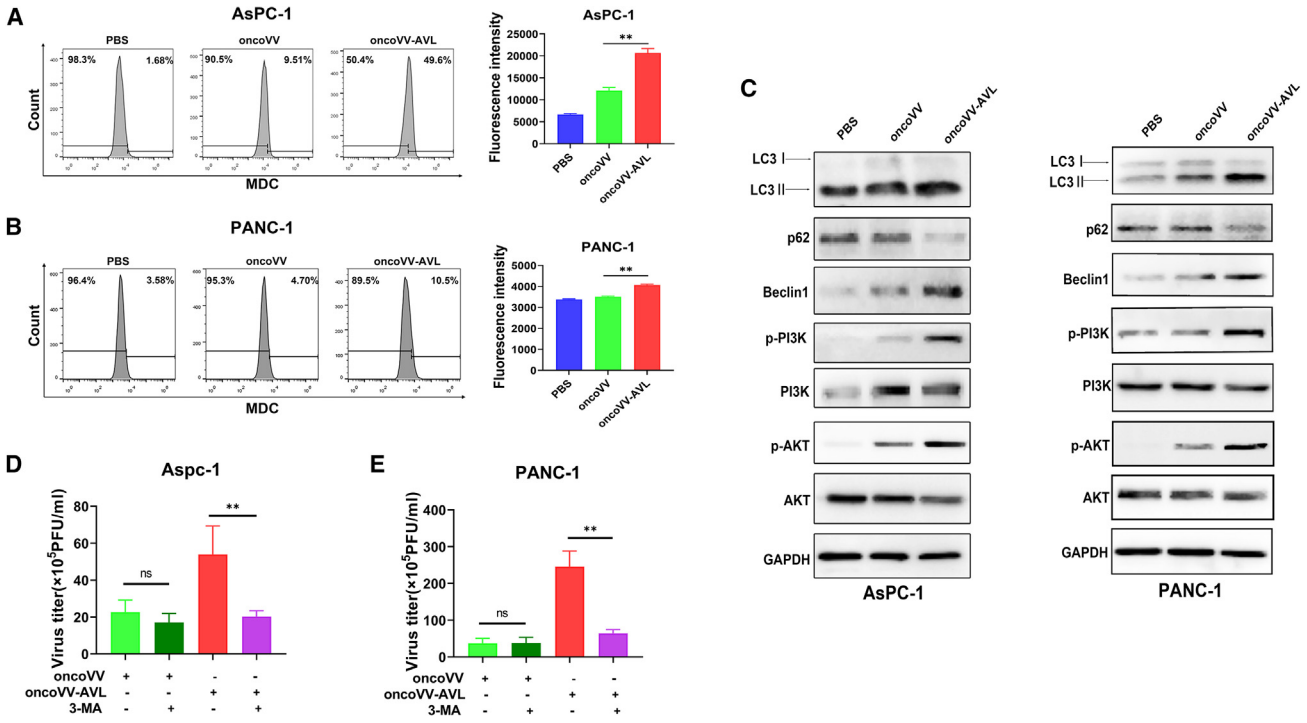

Figure 5. OncoVV-AVL promotes viral replication by eliciting autophagy

(A and B) Quantification of autophagy cells. AsPC-1 (A) and PANC-1 (B) cells were infected with oncoVV or oncoVV-AVL and stained via MDC. (C) Protein expression of LC3I/II, p62, Beclin-1, PI3K, p-PI3K, AKT, and *p*-AKT in PANC-1 and AsPC-1 cells. Western blotting was conducted at 36 h post-oncoVV-AVL infection; GAPDH was used as a loading control. (D and E) Viral replication in the presence of 3-MA. After treatment with 3-MA in AsPC-1 (D) and PANC-1 (E) cells, the viral replication was analyzed. Data are presented as mean ± SD of three independent experiments ($n = 3$). $^{**}p < 0.01$.

DISCUSSION

The development of new interventions for patients with PC is crucial. One promising approach is the utilization of OVs, a novel class of cancer therapeutics that demonstrate significant potential in treating a wide range of cancer types.[48–51] OncoVV-AVL has demonstrated effectiveness against multiple categories of cancer cells. Nevertheless, the underlying mechanism behind its antitumor activity has not yet been elucidated. Here, oncoVV-AVL has demonstrated a strong antitumor effect on PC both *in vivo* and *in vitro*.

There are two primary strategies for OV therapy: direct oncolytic activity through immediate infection and replication, and a delayed effect via the induction of specific antitumor immunity.[52] Viruses, as obligate parasites in cells, have evolved various mechanisms to subvert the host antiviral system and hijack cellular resources to maximize their replication.[53] During the infection process, mitochondria play a crucial role in generating energy, controlling metabolism, and producing ROS.[54] Increasing evidence illustrates that elevated levels of ROS may benefit virus replication by influencing oxidative modifications of viral proteins and modulating host signaling pathways. It has been established that oncolytic Newcastle disease virus extensively alters carbohydrate metabolism through mitophagy and boosts intracellular ROS levels to support viral replication.[35,36] Similarly, recent studies have shown that enterovirus 71 (EV-A71) harnesses the oxidative stress response to facilitate its reproduction and dissemination of viral progeny.[34] Elevated ROS levels have been found to reduce Nrf2 levels and activate endoplasmic reticulum stress autophagy signaling pathways, which can be mitigated by ROS scavengers, resulting in reduced EV-A71 replication.[55,56] Consistent with these conclusions, the present study reveals that oncoVV-AVL infection triggers the significant production of ROS, promoting viral replication and inducing autophagy. Additionally, previous research has demonstrated that ROS predominantly regulate mitochondrial cytochrome *c* and induce apoptosis. In line with this notion, our results indicate that oncoVV-AVL enhances apoptosis by elevating ROS levels, thereby exerting an antitumor effect. In summary, our observations suggest that the production of ROS triggered by oncoVV-AVL infection promotes viral replication, reinforces cell apoptosis, and ultimately enhances the antitumor effect.

PC is characterized by an immunologically suppressed environment, where immunosuppressive cells like myeloid-derived suppressor cells, regulatory T cells, and TAMs are dominant.[57] Notably, TAMs, as the most abundant inflammatory cells in the TME, play a pivotal role in modulating immune cell function, tumor progression, and response to therapy.[58] In the TME, TAMs can dynamically transform between M1 and M2 types, while M1 and M2

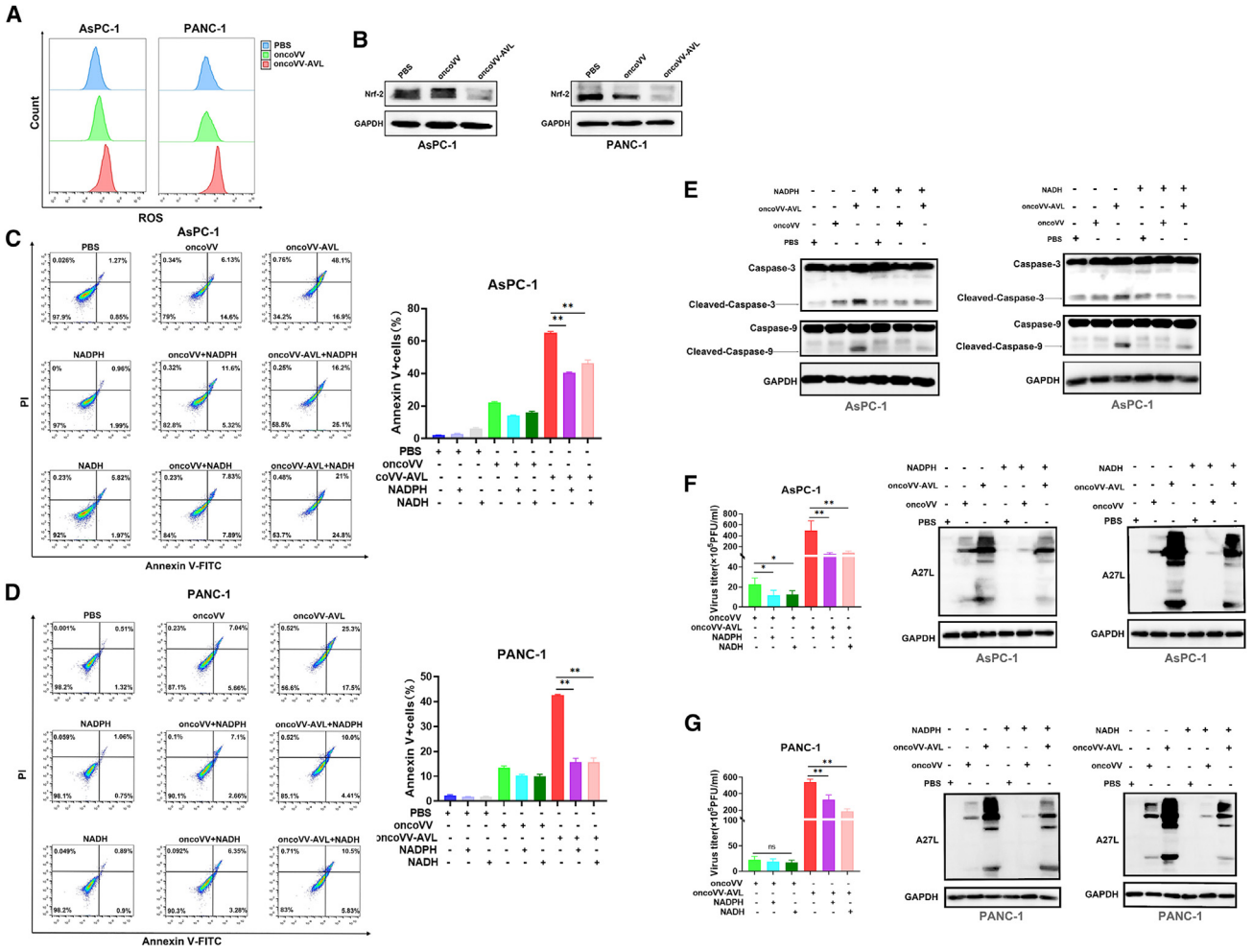

Figure 6. OncoVV-AVL induces oxidative stress in PC cells

(A) Detection of ROS. Levels of ROS were evaluated in PC cells after infection with oncoVV-AVL for 36 h. (B) The expression of Nrf-2 in PC cells. Apoptosis proportion in AsPC-1 (C) and PANC-1 (D) cells' treatment with ROS scavengers. Data are presented as the mean ± SD ($n = 3$). (E) Western blotting detection of apoptosis-related proteins. (F and G) Viral yields in the presence of ROS scavengers. AsPC-1 (F) and PANC-1 (G) cells were treated with NADPH or NADH, followed by oncoVV or oncoVV-AVL infection. A27L and GAPDH protein levels were detected via western blotting in PC cells.

have the opposite function, the former is tumor-suppressing macrophage. Higher ratios of M1 macrophages are associated with longer survival in pancreatic adenocarcinoma.[59] Approaches to reprogram TAMs from M2 to M1 are actively being pursued, with IFN-γ known to induce polarization toward M1-like macrophages.[60] Additionally, ROS generated from mitochondria can directly reinforce the production of inflammatory cytokines through distinct pathways.[61] Based on this, we hypothesize that the activation of ROS by oncoVV-AVL would induce IFN-γ production, leading to M1 polarization. In both BALB/c nude mice and C57BL/6 mice, we observed an increase in IFN-γ levels in oncoVV-AVL treatment, which decreased following the addition of an ROS neutralizer. The increase in IFN-γ levels in the oncoVV-AVL group was significantly more pronounced in nude mice compared to their controls. Conversely, in C57BL/6 mice, although IFN-γ levels were also promoted, there was no statistically significant difference between oncoVV-AVL treatment and controls. We hypothesized that C57BL/6 mice may have a variety of immune cells within them that regulate one another, forcing even a rise in IFN-γ to be insignificant. Notably, macrophages from either BALB/c nude mice or C57BL/6 mice differentiated significantly toward the M1 type, indicating that oncoVV-AVL induces the polarization of M1-type cells and promotes the M1/M2 ratio. OncoVV-AVL triggers antitumor immunity and enhances the activation of M1-polarized macrophages.

In summary, we have shown that oncoVV-AVL enhances antitumor efficacy against PC tumors by mediating ROS-induced viral replication, promoting M1 polarization, and modulating the TME to convert cold PC tumors into hot ones. This suggests that oncoVV-AVL could serve as a novel therapeutic approach to overcome PC tumors.

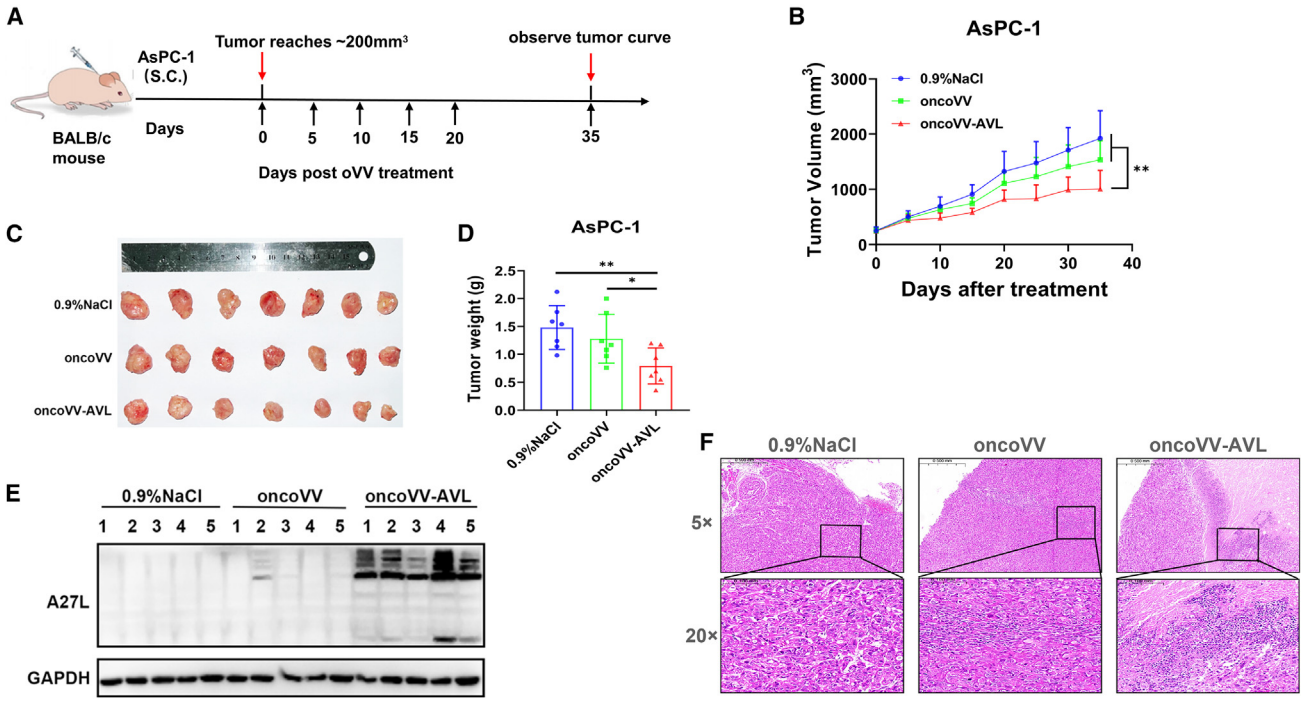

Figure 7. OncoVV-AVL suppressed PC growth in xenograft tumor model

(A) The experimental schedule. (B) Tumor volume curve. The measurement of tumor volume occurred at 5-day intervals. Data are expressed as mean tumor volume ± SD (n = 7). (C) Comparison of tumor size. At the end of the experiment, tumor weights were compared among groups. (D) Tumor weight. Harvested tumor tissues were weighed. Data are presented as the mean ± SD (n = 7). (E) Expression of A27L determined by western blotting. (F) Pathological analysis of tumor tissue.

MATERIALS AND METHODS

Cell culture

HEK293A, human PC cell lines AsPC-1 and PANC-1, and mouse cell line Pan02 used in this investigation were sourced from the Chinese Academy of Sciences. AsPC-1 cells were cultured in RPMI-1640 medium with a concentration of 100 U/mL penicillin and 100 μg/mL streptomycin solution and supplemented with 10% fetal bovine serum (FBS), under a 5% CO_2 environment at 37°C. Likewise, the PANC-1 and HEK293A cells were cultivated in DMEM under identical conditions. The Pan02 cells were cultured in DMEM in combination with 5% FBS and 100 U/mL penicillin and 100 μg/mL streptomycin.

Cell viability assay

AsPC-1 and PANC-1 cells were plated in 96-well plates with a density of 1×10^4 cells per well and cultured for 12 h. Following infection with oncolytic VVs for 24, 48, and 72 h, the cells were collected and assessed using the MTT assay. PBS served as the control, while the cells were infected with oncolytic VV at different MOI levels—1, 2, or 5. Cell viability was determined by adding MTT solution (5 mg/mL) to each well and incubating at 37°C for 4 h. Subsequently, the liquid was aspirated, and DMSO was added to each well and mixed thoroughly on an oscillation instrument for 10 min. The measurement was conducted with a microplate reader (Multiskan, Thermo Scientific, Waltham, MA).

Flow cytometer assay

To assess apoptosis, cells were stained using the FITC Annexin V Apoptosis Detection Kit (BD Biosciences, San Jose, CA) following the guidelines provided by the manufacturer. For ROS analysis, cells were washed with cold PBS and treated with a diluted solution of diacetyldichlorofluorescein (1:10,000; CA1410, Solarbio, Beijing, China) for 15 min at 37°C in a cell culture chamber. After digestion with pancreatic enzyme, the cells were collected and analyzed. To measure autophagy, cells were stained with an Autophagy Staining Assay Kit containing MDC (C3018; Beyotime Biotech, Jiangsu, China) for 30 min. Following digestion with pancreatic enzyme, cells were washed three times with 1× assay buffer.

To detect cell types in mice, AsPC-1 cells (8×10^6 cells) and Pan02 cells (1×10^7 cells) were injected intradermally into the right flanks of BALB/c nude mice or C57BL/6 mice, respectively. Mice bearing subcutaneous tumors were intratumorally treated with 0.9% NaCl, oncoVV, or oncoVV-AVL (1×10^7 PFU per tumor). After 2 weeks of treatment, the mice were sacrificed. Myeloid cells were obtained from the femurs and tibiae of donor mice. The cell suspensions were passed through a 300-mesh nylon filter and washed twice with 1% FBS in PBS. Erythrocytes were eliminated by incubating with RBC Lysis Buffer (420302; BioLegend, San Diego, CA). The single-cell suspension was stained with the flow cytometry antibodies listed in Schedule 3. All washes and staining procedures were carried out

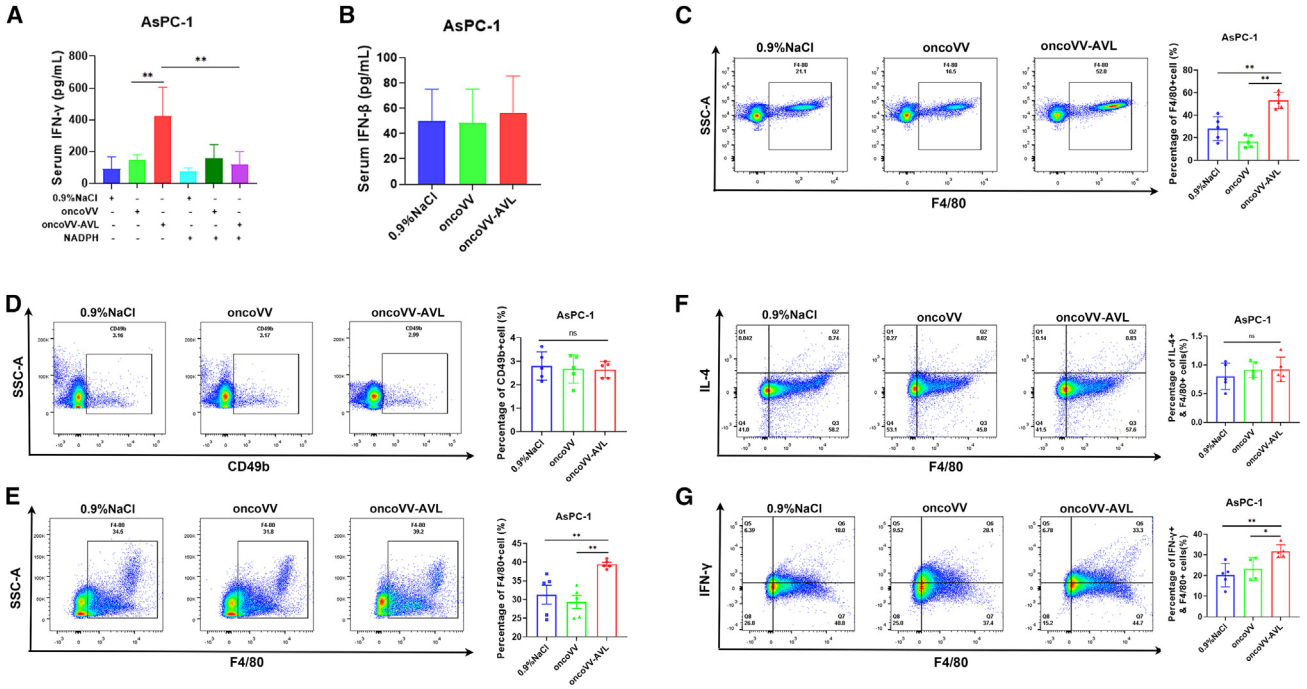

Figure 8. OncoVV-AVL induced antitumor immunity in BALB/c nude mice

(A and B) Cytokines IFN-γ/-β in the mouse serum. Cytokines were detected by ELISA kit. (C) Peritoneal exudate cell analysis. Percentage of F4/80$^+$ cells in peritoneal exudate cells was analyzed by flow cytometry. (D and E) Myeloid cells analysis. Percentage of CD49b$^+$ cells and F4/80$^+$ cells for detection in the myeloid cells by flow cytometry. (F and G) Polarization of macrophages. Percentages of IFN-γ$^+$, IL-4$^+$ within the F4/80$^+$ cells in each group. All data are presented as mean ± SD ($n = 5$). *$p < 0.05$; **$p < 0.01$.

using 1% FBS in PBS. Subsequently, the samples were analyzed using a BD Fortessa flow cytometer (C6; BD Biosciences) and FlowJo10 software.

Detection of viral replication ability

To detect viral reproduction in PC cells, cells were seeded onto 24-well plates and infected with either oncoVV or oncoVV-AVL after cultivation for 12 h in a cell incubator. Samples were gathered at various time intervals (0, 24, and 36 h post-infection) and subjected to three rounds of freeze-thaw processes alternating between −80°C and room temperature (RT). The viral titer was determined using a $TCID_{50}$ assay with 293A cells. For investigating the influence of autophagy on viral replication, the virus-infected cells were treated with 3-MA (400 μM; S2767; Selleck Chemicals, Houston, TX). To study viral replication influenced by ROS, PC cells were co-cultured with NADPH (300 μM; HY-F0003; MCE, Monmouth Junction, NJ) or NADH (100 μM; S6349; Selleck Chemicals) as part of the experimental design.

Western blotting

Cells 36 h post-infection were gathered, homogenized, quantified, and electrophoresed by 12% SDS-PAGE. Proteins were electroblotted onto a polyvinylidene fluoride membrane. The membranes were immersed in a solution of 5% skim milk at RT for 2 h and then incubated at 4°C overnight using the primary antibodies listed in Table S1. After washes with TBS-T (TBS with 0.1% Tween 20) three times, the membranes were stained with corresponding secondary antibody for 1.5 h at RT. Following another three washes, the blots were visualized utilizing enhanced chemiluminescence substrate (RM00021; ABclonal, New Taipei City, Taiwan) and scanned with a chemiluminescence imaging system.

qPCR

The PANC-1 and AsPC-1 cells were seeded in triplicate into 24-well plates and infected with the viruses for 36 h. Total RNA was separated utilizing the RNA-Quick Purification Kit (RN001; ES Science, Shanghai, China), followed by reverse transcription into cDNA using the ReverTra Ace qPCR RT Kit (FSQ-101; Toyobo, Osaka, Japan). Approximately 5 ng of cDNA was amplified using the SYBR Green Real-time PCR Master Mix (QPK-201; Toyobo,) following the instructions provided by the manufacturer. The expression levels of each gene were standardized adopting glyceraldehyde 3-phosphate dehydrogenase (GAPDH) as a reference, and mRNA expression was analyzed using comparative Ct (cycle threshold) values. A tabulation of qPCR primers used in this study is described in Table S2.

Dual-luciferase reporter gene assay

Following a 12-h incubation of AsPC-1 and PANC-1 cells in a 96-well microplate (655080; Greiner Bio-One, Monroe, NC), the Renilla luciferase reporter vector PRL-TK and plasmids carrying the target genes (IRF-3, IRF-7, AP-1) were introduced into the cells via co-transfection at a mass ratio of 1:500. The PRL-TK vector was used

as an internal control. Following 4–6 h of co-transfection, the media was partially replaced, and the cells were further incubated for 24 h. Subsequently, PC cells were subjected to treatment with PBS, oncoVV, or oncoVV-AVL at an MOI of 2 for 36 h. Following the instructions, luciferase activity was measured utilizing a chemiluminescence instrument with the Dual-Glo Luciferase Assay System (E2920; Promega, Madison, WI). Finally, the ratio of luminescence from the experimental reporter to that from the control reporter was computed.

Tumor growth experiments

Female BALB/c nude mice (6 weeks old) were obtained from SLAC Laboratory Animal Company (Shanghai, China) and were subcutaneously injected with 8×10^6 AsPC-1 cells into the right axilla. These mice were allocated a conventional diet and resided in an environment free from specific pathogens. Once the tumor size reached around 200 mm^3, the mice were assigned randomly to one of three treatment groups (n = 7/group). Each mouse in the blank control group, negative control group, and experimental group received injections of 100 μL physiological saline, 1×10^7 PFU oncoVV, or oncoVV-AVL. Tumor volume was monitored every 5 days using calipers and calculated using the formula half the length multiplied by the square of the width. After 35 days, the mice were humanely euthanized by cervical dislocation. The tumors were harvested, fixed with 4% formalin, and used for downstream analysis as mentioned above. All animal experiments at Zhejiang Sci-Tech University were sanctioned by the Ethics Committee for Animal Experimentation.

H&E staining

AsPC-1 tumor tissues were separated subcutaneously from the euthanized tumor-bearing mice, immersed in 4% paraformaldehyde for 48 h, and preserved in 75% ethanol. Paraffin-embedded sections were prepared and stained with H&E to assess the tumor regions. The histological analysis was carried out by HaoKe Biotechnology Company (Hangzhou, China), and sections were observed under a microscope.

ELISA

On the 14th day of treatment with oncoVV or oncoVV-AVL, blood samples were collected from the mouse's orbit and centrifuged to obtain the mouse serum. The concentration of IFN-β or IFN-γ in the serum was detected utilizing the Mouse IFN-β ELISA Kit (EK2236; Multi Science, Hangzhou, China) and the Mouse IFN-γ ELISA Kit (EK280; Multi Science), following the instructions.

Data analysis

Statistical analysis was performed using GraphPad Prism 8.0 (GraphPad Software, San Diego, CA). The one-way ANOVA test was performed for comparison among groups. All results were shown in mean ± SD, and $*p < 0.05$ or $**p < 0.01$ was considered statistically significant; ns indicated no significance.

DATA AND CODE AVAILABILITY

All the data that support the findings of this study are available from the corresponding authors upon reasonable request.

ACKNOWLEDGMENTS

Funding for this research project was provided by the National Natural Science Foundation of China (grant no. 42376105), Natural Science Foundation of Zhejiang Province (grant no. LTGY23D060001). All animal experiments at Zhejiang Sci-Tech University were sanctioned by the Ethics Committee for Animal Experimentation (no. 202110302-1).

AUTHOR CONTRIBUTIONS

All authors contributed to the study conception and design. G.L. conceived and supervised this study. Material preparation, data collection, and analysis were performed by J.Y. and T.Y. The first draft of the manuscript was written by T.Y and J.Y. All authors have read and agreed to the published version of the manuscript.

DECLARATION OF INTERESTS

The authors declare no competing interests.

SUPPLEMENTAL INFORMATION

Supplemental information can be found online at https://doi.org/10.1016/j.omton.2024.200878.

REFERENCES

1. Siegel, R.L., Miller, K.D., Fuchs, H.E., and Jemal, A. (2022). Cancer statistics, 2022. CA. Cancer J. Clin. *72*, 7–33.
2. Kamisawa, T., Wood, L.D., Itoi, T., and Takaori, K. (2016). Pancreatic cancer. Lancet *388*, 73–85.
3. Ryan, D.P., Hong, T.S., and Bardeesy, N. (2014). Pancreatic adenocarcinoma. N. Engl. J. Med. *371*, 1039–1049.
4. Vincent, A., Herman, J., Schulick, R., Hruban, R.H., and Goggins, M. (2011). Pancreatic cancer. Lancet *378*, 607–620.
5. Liu, L., Kshirsagar, P.G., Gautam, S.K., Gulati, M., Wafa, E.I., Christiansen, J.C., White, B.M., Mallapragada, S.K., Wannemuehler, M.J., Kumar, S., et al. (2022). Nanocarriers for pancreatic cancer imaging, treatments, and immunotherapies. Theranostics *12*, 1030–1060.
6. Neoptolemos, J.P., Kleeff, J., Michl, P., Costello, E., Greenhalf, W., and Palmer, D.H. (2018). Therapeutic developments in pancreatic cancer: current and future perspectives. Nat. Rev. Gastroenterol. Hepatol. *15*, 333–348.
7. Ansari, D., Tingstedt, B., Andersson, B., Holmquist, F., Sturesson, C., Williamsson, C., Sasor, A., Borg, D., Bauden, M., and Andersson, R. (2016). Pancreatic cancer: yesterday, today and tomorrow. Future Oncol. *12*, 1929–1946.
8. Sun, D., Ma, J., Wang, J., Zhang, F., Wang, L., Zhang, S., Chen, G., Li, X., Du, W., Cui, P., and Hu, Y. (2018). Clinical observation of immune checkpoint inhibitors in the treatment of advanced pancreatic cancer: a real-world study in Chinese cohort. Ther. Clin. Risk Manag. *14*, 1691–1700.
9. Kelly, E., and Russell, S.J. (2007). History of oncolytic viruses: genesis to genetic engineering. Mol. Ther. *15*, 651–659.
10. Tian, Y., Xie, D., and Yang, L. (2022). Engineering strategies to enhance oncolytic viruses in cancer immunotherapy. Signal Transduct. Target. Ther. *7*, 117.
11. Huang, Z., Guo, H., Lin, L., Li, S., Yang, Y., Han, Y., Huang, W., and Yang, J. (2023). Application of oncolytic virus in tumor therapy. J. Med. Virol. *95*, e28729.
12. Ma, R., Li, Z., Chiocca, E.A., Caligiuri, M.A., and Yu, J. (2023). The emerging field of oncolytic virus-based cancer immunotherapy. Trends Cancer *9*, 122–139.
13. Bommareddy, P.K., Shettigar, M., and Kaufman, H.L. (2018). Integrating oncolytic viruses in combination cancer immunotherapy. Nat. Rev. Immunol. *18*, 498–513.
14. Russell, S.J., and Peng, K.W. (2017). Oncolytic Virotherapy: A Contest between Apples and Oranges. Mol. Ther. *25*, 1107–1116.
15. Yoon, A.R., Hong, J., Jung, B.K., Ahn, H.M., Zhang, S., and Yun, C.O. (2023). Oncolytic adenovirus as pancreatic cancer-targeted therapy: Where do we go from here? Cancer Lett. *579*, 216456.
16. West, E.J., Scott, K.J., Tidswell, E., Bendjama, K., Stojkowitz, N., Lusky, M., Kurzawa, M., Prasad, R., Toogood, G., Ralph, C., et al. (2022). Intravenous Oncolytic Vaccinia

Virus Therapy Results in a Differential Immune Response between Cancer Patients. Cancers *14*, 2181.

17. Torres-Domínguez, L.E., and McFadden, G. (2019). Poxvirus oncolytic virotherapy. Expert Opin. Biol. Ther. *19*, 561–573.
18. McFadden, G. (2005). Poxvirus tropism. Nat. Rev. Microbiol. *3*, 201–213.
19. Holloway, R.W., Mendivil, A.A., Kendrick, J.E., Abaid, L.N., Brown, J.V., LeBlanc, J., McKenzie, N.D., Mori, K.M., and Ahmad, S. (2023). Clinical activity of olvimulogene Nanivacirepvec-Primed immunochemotherapy in heavily pretreated patients with platinum-resistant or platinum-refractory ovarian cancer: The Nonrandomized Phase 2 VIRO-15 Clinical Trial. JAMA Oncol. *9*, 903–908.
20. Toulmonde, M., Guegan, J.P., Spalato-Ceruso, M., Peyraud, F., Kind, M., Vanhersecke, L., Le Loarer, F., Perret, R., Cantarel, C., Bellera, C., et al. (2024). Reshaping the tumor microenvironment of cold soft-tissue sarcomas with oncolytic viral therapy: a phase 2 trial of intratumoral JX-594 combined with avelumab and low-dose cyclophosphamide. Mol. Cancer *23*, 38.
21. Gautam, A.K., Sharma, D., Sharma, J., and Saini, K.C. (2020). Legume lectins: potential use as a diagnostics and therapeutics against the cancer. Int. J. Biol. Macromol. *142*, 474–483.
22. Yau, T., Dan, X., Ng, C.C.W., and Ng, T.B. (2015). Lectins with potential for anti-cancer therapy. Molecules *20*, 3791–3810.
23. Catanzaro, E., Calcabrini, C., Bishayee, A., and Fimognari, C. (2019). Antitumor potential of marine and freshwater lectins. Mar. Drugs *18*, 11.
24. Cheung, R.C.F., Wong, J.H., Pan, W., Chan, Y.S., Yin, C., Dan, X., and Ng, T.B. (2015). Marine lectins and their medicinal applications. Appl. Microbiol. Biotechnol. *99*, 3755–3773.
25. Yang, X., Wu, L., Duan, X., Cui, L., Luo, J., and Li, G. (2014). Adenovirus carrying gene encoding haliotis discus discus sialic acid binding lectin induces cancer cell apoptosis. Mar. Drugs *12*, 3994–4004.
26. Zhou, Y., Wang, Q., Ying, Q., Zhang, X., Chen, K., Ye, T., and Li, G. (2023). Effects of oncolytic vaccinia viruses harboring different marine lectins on hepatocellular carcinoma cells. Int. J. Mol. Sci. *24*, 3823.
27. Zhou, Y., Wang, Q., Ying, Q., Zhang, X., Ye, T., Chen, K., and Li, G. (2023). A comparative study of oncolytic vaccinia viruses harboring different marine lectins in breast cancer Cells. Mar. Drugs *21*, 77.
28. Wu, T., Xiang, Y., Liu, T., Wang, X., Ren, X., Ye, T., and Li, G. (2019). Oncolytic vaccinia virus expressing aphrocallistes vastus lectin as a cancer therapeutic agent. Mar. Drugs *17*, 363.
29. Vázquez, M.I., Rivas, G., Cregut, D., Serrano, L., and Esteban, M. (1998). The vaccinia virus 14-kilodalton (A27L) fusion protein forms a triple coiled-coil structure and interacts with the 21-kilodalton (A17L) virus membrane protein through a C-terminal alpha-helix. J. Virol. *72*, 10126–10137.
30. Smith, G.L., Talbot-Cooper, C., and Lu, Y. (2018). How does vaccinia virus interfere with interferon? Adv. Virus Res. *100*, 355–378.
31. Aaronson, D.S., and Horvath, C.M. (2002). A road map for those who don't know JAK-STAT. Science *296*, 1653–1655.
32. Chaudhary, M.R., Chaudhary, S., Sharma, Y., Singh, T.A., Mishra, A.K., Sharma, S., and Mehdi, M.M. (2023). Aging, oxidative stress and degenerative diseases: mechanisms, complications and emerging therapeutic strategies. Biogerontology *24*, 609–662.
33. Ying, W. (2008). NAD+/NADH and NADP+/NADPH in cellular functions and cell death: regulation and biological consequences. Antioxid. Redox Signal. *10*, 179–206.
34. Cheng, M.L., Weng, S.F., Kuo, C.H., and Ho, H.Y. (2014). Enterovirus 71 induces mitochondrial reactive oxygen species generation that is required for efficient replication. PLoS One *9*, e113234.
35. Gong, Y., Tang, N., Liu, P., Sun, Y., Lu, S., Liu, W., Tan, L., Song, C., Qiu, X., Liao, Y., et al. (2022). Newcastle disease virus degrades SIRT3 via PINK1-PRKN-dependent mitophagy to reprogram energy metabolism in infected cells. Autophagy *18*, 1503–1521.
36. Tang, N., Chen, P., Zhao, C., Liu, P., Tan, L., Song, C., Qiu, X., Liao, Y., Liu, X., Luo, T., et al. (2023). Newcastle disease virus manipulates mitochondrial MTHFD2-mediated nucleotide metabolism for virus replication. J. Virol. *97*, e0001623.
37. Billiau, A., and Matthys, P. (2009). Interferon-gamma: a historical perspective. Cytokine Growth Factor Rev. *20*, 97–113.
38. Jorgovanovic, D., Song, M., Wang, L., and Zhang, Y. (2020). Roles of IFN-γ in tumor progression and regression: a review. Biomark. Res. *8*, 49.
39. Thibaut, R., Bost, P., Milo, I., Cazaux, M., Lemaître, F., Garcia, Z., Amit, I., Breart, B., Cornuot, C., Schwikowski, B., and Bousso, P. (2020). Bystander IFN-γ activity promotes widespread and sustained cytokine signaling altering the tumor microenvironment. Nat. Cancer *1*, 302–314.
40. Basu, A., Ramamoorthi, G., Albert, G., Gallen, C., Beyer, A., Snyder, C., Koski, G., Disis, M.L., Czerniecki, B.J., and Kodumudi, K. (2021). Differentiation and regulation of T(H) cells: a balancing act for cancer immunotherapy. Front. Immunol. *12*, 669474.
41. Benci, J.L., Xu, B., Qiu, Y., Wu, T.J., Dada, H., Twyman-Saint Victor, C., Cucolo, L., Lee, D.S.M., Pauken, K.E., Huang, A.C., et al. (2016). Tumor interferon signaling regulates a multigenic resistance program to immune checkpoint blockade. Cell *167*, 1540–1554.e12.
42. Bejarano, L., Jordão, M.J.C., and Joyce, J.A. (2021). Therapeutic targeting of the tumor microenvironment. Cancer Discov. *11*, 933–959.
43. Bilotta, M.T., Antignani, A., and Fitzgerald, D.J. (2022). Managing the TME to improve the efficacy of cancer therapy. Front. Immunol. *13*, 954992.
44. Timmer, F.E.F., Geboers, B., Nieuwenhuizen, S., Dijkstra, M., Schouten, E.A.C., Puijk, R.S., de Vries, J.J.J., van den Tol, M.P., Bruynzeel, A.M.E., Streppel, M.M., et al. (2021). Pancreatic cancer and immunotherapy: a clinical overview. Cancers *13*, 4138.
45. Vitale, I., Manic, G., Coussens, L.M., Kroemer, G., and Galluzzi, L. (2019). Macrophages and metabolism in the tumor microenvironment. Cell Metab. *30*, 36–50.
46. Haidl, I.D., and Jefferies, W.A. (1996). The macrophage cell surface glycoprotein F4/80 is a highly glycosylated proteoglycan. Eur. J. Immunol. *26*, 1139–1146.
47. Walzer, T., Jaeger, S., Chaix, J., and Vivier, E. (2007). Natural killer cells: from CD3(-) NKp46(+) to post-genomics meta-analyses. Curr. Opin. Immunol. *19*, 365–372.
48. Liu, S., Li, F., Ma, Q., Du, M., Wang, H., Zhu, Y., Deng, L., Gao, W., Wang, C., Liu, Y., et al. (2023). OX40L-armed oncolytic virus boosts T-cell response and remodels tumor microenvironment for pancreatic cancer treatment. Theranostics *13*, 4016–4029.
49. Wang, R., Chen, J., Wang, W., Zhao, Z., Wang, H., Liu, S., Li, F., Wan, Y., Yin, J., Wang, R., et al. (2022). CD40L-armed oncolytic herpes simplex virus suppresses pancreatic ductal adenocarcinoma by facilitating the tumor microenvironment favorable to cytotoxic T cell response in the syngeneic mouse model. J. Immunother. Cancer *10*, e003809.
50. Zhu, Z., McGray, A.J.R., Jiang, W., Lu, B., Kalinski, P., and Guo, Z.S. (2022). Improving cancer immunotherapy by rationally combining oncolytic virus with modulators targeting key signaling pathways. Mol. Cancer *21*, 196.
51. Guo, Z.S., Lotze, M.T., Zhu, Z., Storkus, W.J., and Song, X.T. (2020). Bi- and tri-specific T cell engager-armed oncolytic viruses: next-generation cancer immunotherapy. Biomedicines *8*, 204.
52. Cook, M., and Chauhan, A. (2020). Clinical application of oncolytic viruses: a systematic review. Int. J. Mol. Sci. *21*, 7505.
53. Passalacqua, K.D., Lu, J., Goodfellow, I., Kolawole, A.O., Arche, J.R., Maddox, R.J., Carnahan, K.E., O'Riordan, M.X.D., and Wobus, C.E. (2019). Glycolysis is an intrinsic factor for optimal replication of a norovirus. mBio *10*, e02175-18.
54. Foo, J., Bellot, G., Pervaiz, S., and Alonso, S. (2022). Mitochondria-mediated oxidative stress during viral infection. Trends Microbiol. *30*, 679–692.
55. You, L., Chen, J., Liu, W., Xiang, Q., Luo, Z., Wang, W., Xu, W., Wu, K., Zhang, Q., Liu, Y., and Wu, J. (2020). Enterovirus 71 induces neural cell apoptosis and autophagy through promoting ACOX1 downregulation and ROS generation. Virulence *11*, 537–553.
56. Du, N., Li, X.H., Bao, W.G., Wang, B., Xu, G., and Wang, F. (2019). Resveratrol-loaded nanoparticles inhibit enterovirus 71 replication through the oxidative stress-mediated ERS/autophagy pathway. Int. J. Mol. Med. *44*, 737–749.

57. Li, Y., Xiang, S., Pan, W., Wang, J., Zhan, H., and Liu, S. (2023). Targeting tumor immunosuppressive microenvironment for pancreatic cancer immunotherapy: Current research and future perspective. Front. Oncol. *13*, 1166860.

58. Christofides, A., Strauss, L., Yeo, A., Cao, C., Charest, A., and Boussiotis, V.A. (2022). The complex role of tumor-infiltrating macrophages. Nat. Immunol. *23*, 1148–1156.

59. Rosenberg, A., and Mahalingam, D. (2018). Immunotherapy in pancreatic adenocarcinoma-overcoming barriers to response. J. Gastrointest. Oncol. *9*, 143–159.

60. Mily, A., Kalsum, S., Loreti, M.G., Rekha, R.S., Muvva, J.R., Lourda, M., and Brighenti, S. (2020). Polarization of M1 and M2 human monocyte-derived cells and analysis with flow cytometry upon mycobacterium tuberculosis infection. J. Vis. Exp. *163*, e61807.

61. Chatterjee, S., Balram, A., and Li, W. (2021). Convergence: Lactosylceramide-centric signaling pathways induce inflammation, oxidative stress, and other phenotypic outcomes. Int. J. Mol. Sci. *22*, 1816.